Electrocatalysis (2023) 14:88–97
https://doi.org/10.1007/s12678-022-00777-9

ORIGINAL RESEARCH

Carbon-Based Electrochemical Sensor for the Detection and Degradation of Persistent Toxic Carbendazim in Soil and Water Sample

Keerthi Prabhu[1] · **Shweta J. Malode**[2] · **Nagaraj P. Shetti**[2]

Accepted: 19 September 2022 / Published online: 29 September 2022

Abstract

The carbendazim (CBM) electrochemical performance was analyzed using a glassy carbon electrode (GCE) in a 0.2 M phosphate buffer solution. An enhanced peak current of CBM was observed at GCE when the surface was modified with Vat Violet 2R (VVR) dye. The VVR was electro-polymerized on the GCE surface utilizing voltammetric techniques. The constructed GCE presented excellent electrocatalytic behavior for the electro-oxidation of CBM in a 0.2 M PB of 3.0 pH. A well-resolved peak of the CBM with enhancement in the current was obtained for the developed GCE. The impact of electroanalytical parameters such as accumulation time, temperature variation, pH, heterogeneous rate, sweep rate, activation energy, transfer coefficient, and the total number of electrons and protons transferred have been evaluated. Like water and soil, the actual samples were investigated using voltammetric techniques. The developed sensor is sensitive for analyzing CBM through detection and quantification limits of CBM.

Keywords Carbendazim · Electrochemical behavior · Glassy carbon electrode · Sample analysis · Environmental applications

Introduction

Electroanalytical methods have drawn researchers' interest in the advancement of electrochemical sensors to examine electroactive molecules [1–3]. Voltammetric procedures have been extensively incorporated over the past few decades because of their ease of use, low price, excellent sensitivity, and rapid response [4, 5]. Carbon electrodes have been extensively employed for electrochemical studies of oxidizable substances [6]. One of its essential properties is the electrode's catalytic function due to the electrode surface. Many surface modification approaches enhance the electrocatalytic behavior of an electrode. By adopting nanoparticles [7, 8], conducting polymer layers [9], nanotubes [10], and ionic liquids [11], the modification may be accomplished. Due to their enhanced physicochemical characteristics, including electrocatalysis throughout the redox mechanism, working electrodes covered with electro-polymerized conducting polymer layers have been essential [12, 13]. Electro-polymerization is a process that has many benefits, such as making the organic molecule immobilized evenly. By altering the electroanalytical parameters, film thickness could be easily managed, and more extended period stability of activity and charge transfer features could be achieved [14]. Several research experiments have shown that polymer film fabricated electrodes have improved reactions in identifying specific electroactive substances. Specifically, dyestuff polymerization may develop cross-linked oligomers, improving adsorption capacity [15].

In recent decades, intensive pesticide use has boosted agricultural output. However, at the same time, it has produced pesticides that rest in earthy water streams at points that go outside the judicial confines and have intensified risk complications in the atmosphere and nutrient security concerns [16]. Indeed, many chemicals are almost

✉ Shweta J. Malode
shweta.malode@kletech.ac.in

✉ Nagaraj P. Shetti
dr.npshetti@gmail.com

[1] Department of Chemistry, K.L.E. Institute of Technology, Hubballi 580027, Karnataka, India

[2] Department of Chemistry, School of Advanced Sciences, KLE Technological University, Vidyanagar 580031, Karnataka, India

non-biodegradable, but these can be observable in soil, water bodies, air, and food supplies [17, 18]. There might be a significant risk of health complications such as respiratory issues, infertility, immunological issues, bone marrow defects, neurological abnormalities, and cytogenetic consequences owing to the toxic effect of the pesticide [19–21]. A benzimidazole fungicide, carbendazim (CBM), has been extensively utilized to prevent fungal infections and eliminate germs that damage the fruits and veggies in the food supply chain [10]. When two fungicides, benomyl (methyl 1-(butyl carbamoyl)benzimidazole-2-ylcaxbamate) and thiophanate-methyl [dimethyl 4,4′-(o-phenylene) bis(3-thioallophanate)], are sprinkled on field crops, they degrade to carbendazim and interact with water and damp soil [22]. When such two fungicides are converted into CBM for a short period, carbendazim (CBM) remains in the crops, water, and soil for a longer time [22–24]. Thus, CBM is investigated by the existence of its residues. For food products contaminated with carbendazim (fresh fruits and vegetables, oil seeds, cereals, spices, etc.), maximum residue limits (MRLs) have been established by regulatory authorities. For instance, the MRL for carbendazim in fruit juices is 200 ppb, while the European Union has established the MRL for benzimidazole insecticides at 500 ppb. Due to its widespread appeal and the fact that children are their main customers, the introduction of carbendazim in fruit juice products has generated a lot of concern [23]. It has become dangerous to living organisms and the environment because of its gradual degradation [25, 26]. Furthermore, developing low-cost, quick, sensitive, and accurate electrochemical methods is critical for monitoring CBM in general health and environmental pollution [27, 28]. Successively, different techniques for evaluating CBM have been used, including high-performance liquid chromatography [29], capillary electrophoresis [30], photometry method [31], fluorescence study [32], and solid-phase extraction-high-performance liquid chromatography [33]. Such procedures are lengthy and tedious and involve overpriced equipment. Electrochemical techniques attracted us to a larger extent; thus, we preferred the electroanalytical approach.

In the present work, a glassy carbon electrode (GCE) was used to get a CBM response for detection and determination by electro-polymerization of GCE through a cyclic voltammetric method. We have selected Vat Violet 2R (VVR) dye for electro-polymerization on the GCE. Vat Violet 2R is a vat dye that can be dissolved in sodium hydroxide and sodium hydrogen sulfite. It can also be dissolved in water [34]. Vat dyes are rapid to wash and light. It is possible to find bright colors in many other shades [35]. These dyes originated in central Europe; due to the use of vats to reduce indigo plants through the fermentation process, they are specified as vat dyes. These dyes are essential for identifying and dyeing cellulosic fibers and cotton. They appear as direct dyes in their soluble regions so that dyeing can be done on cotton [34]. Using cyclic voltammetry (CV), square wave voltammetry (SWV), and differential pulse voltammetry (DPV), a poly(VVR) glassy carbon electrode, i.e., (poly(VVR)/GCE), demonstrated improved electrochemical performance at pH 3.0.

Experiment

Reagents and Apparatus

A phosphate buffer solution (PB) of an ionic concentration of 0.2 mol/L was prepared as a supporting electrolyte. The required pH from 3.0 to 11.2 was maintained by combining the necessary ratios of Na_2HPO_4 and $NaH_2PO_4{\cdot}H_2O$. The analyte CBM and the modifier Vat Violet 2R have been bought from Sigma-Aldrich, USA. The CBM stock solution (0.1 mM) was prepared in ethanol. The VVR solution was prepared with sodium hydroxide and sodium hydrogen sulfite solution mixture at a temperature of 50 °C by stirring the dye into the mix for 15 to 20 min. For each trial, double-distilled water was employed. Each purchased chemical was of analytical reagent grade and was employed without further refining. Electrochemical investigations were executed using the CHI-D630 model (CH Instrument-D630 electrochemical workstation). In a one-compartment electrode cell, a standard three-electrode system was used with an Ag|AgCl (3.0 M KCl) electrode as a reference, a platinum wire as a counter, and bare and poly(VVR)/GCE as working electrodes. The oxidation potential of the CBM versus the Ag|AgCl electrode has been reported.

Soil Sample

Many types of soil, namely black, brick, lake, farm, and red soil, have been collected from many places. Under the defined earth layers, these soil types were separated, considering sand particles and small and medium to large stones. Later, the collected samples were processed and homogenized. Effectively, a certain amount of soil samples was shifted to a beaker containing 25 mL of distilled water to mix evenly and reserved to remain for about 8–9 h to remove the contaminated part. Similarly, all sample solutions were processed and gathered in a volumetric flask. In addition, a CBM stock solution of 0.1 mM was added to the sample solution and then diluted using double-distilled water. The quantity of CBM is measured using the SWV method, the standard addition method.

Water Sample

Water samples from many places were collected, including a tap, a pond, reverse osmosis (RO), a dam, and a lake. The suspended and colloidal particles were removed from these samples through pre-treatment. SWVs were recorded in both blank and in the presence of a 0.1 mM CBM analyte in water samples. About 5.0 mL of 3.0 pH PB was added to 5.0 mL of a water sample taken in an electrochemical cell to record the voltammograms. Later, water samples of up to 50 mL, a known amount of CBM, i.e., a stock solution of 0.1 mM, were spiked, and SWVs of the water sample were recorded. Following the same procedure, an actual sample voltammogram was obtained. Therefore, the amount of CBM was quantified according to the standard addition method and calibration plot.

Results and Discussion

Surface Area of Electrodes

The cyclic voltammetry method was utilized to determine the surface area of the bare and modified GCE. The test was performed using 1.0 mM $K_4[Fe(CN)_6]$ taken in 0.1 M KCl. The CVs were recorded at different scan rates [5, 36]. Corresponding values of current at different scan rates were noted. The correlation equation of I_p versus $\upsilon^{1/2}$ was substituted into the Randles–Sevcik equation for the reversible reaction, $I_p = (2.69 \times 10^5)\, D_o^{1/2}\, C^*\, A^o\, n^{3/2}\, \upsilon^{1/2}$ at 298 K, and the effective surface area (A^o) was calculated. Here, C^* represents the concentration of $K_4[Fe(CN)_6]$, D_o is the diffusion coefficient of 7.6×10^{-6} cm^2 s^{-1}, I_p is anodic peak current, $\upsilon^{1/2}$ is the square root of scan rate, and n is the total number of electrons involved in the redox reaction of $K_4[Fe(CN)_6]$, i.e., equal to one. The obtained A^o value for modified GCE was nearly twice higher (0.078 cm^2) than bare GCE (0.043 cm^2).

Accumulation Time

Using 0.3 µM of size α-alumina powder, GCE was polished with a wet polishing cloth until a shiny appearance was noticed. In addition to cleaning and activating the GCE surface, ultra-sonication was continuously performed in ethanol with 1:1 nitric acid and double-distilled water. Later, GCE was dehydrated in the nitrogen atmosphere. The 1.0 mM VVR was coated on GCE through electro-polymerization and left to dry to find out the accumulation time. Then, it was dipped in the analyte solution, and later, a CV process was chosen to test against peak current oxidation of 0.1 mM CBM in PB solution to study the accumulation time effect for 0 s and frequent until the 60 s (0, 10, 20, 30, 40, 50, 60) against peak current. In the 40 s, the highest current value was in the voltammogram (Fig. 1). Therefore, the 40 s is considered an appropriate accumulation time to research all parameters in the research work.

Electro-polymerization of VVR on the GCE Surface

After cleaning and activating the GCE, a CV method was used to achieve electro-polymerization of the VVR layer over the GCE. GCE's electrocatalytic activity is also influenced by the degree of thickness of the layer. The poly(VVR) modified glassy carbon electrode (poly(VVR)/GCE) was prepared by adding 1.0 mM VVR with 1.0 M NaOH solution in an electrochemical cell. As demonstrated in Fig. 2A, throughout several cycles (5, 10, 15, 20, and 25), the peak current of CBM increased gradually to 20 cycles, then decreased with cyclic periods. By varying the multiple cycles on the GCE, coverage was controlled. However, at 20 cycles, the peak current was higher. Electro-polymerization was achieved between − 0.6 V and + 1.6 V potential window. As the polymerization cycles are more than 20, the higher currents tend to decrease; increasing the layer thickness will inhibit the electron transport activity and slow the oxidation process. Thus, at 20 cycles, the CV technique was performed for the polymerization of 1.0 mM VVR with 1.0 M NaOH and 1.0 M $NaHSO_3$ solution present in the electrochemical cell with a scanning value of 0.1 V/s with − 0.6 to + 1.6 V potential window (Fig. 2). This shows that the VVR film was developed on the GCE surface. The new poly(VVR)/GCE was used to study the carbendazim fungicide for further studies.

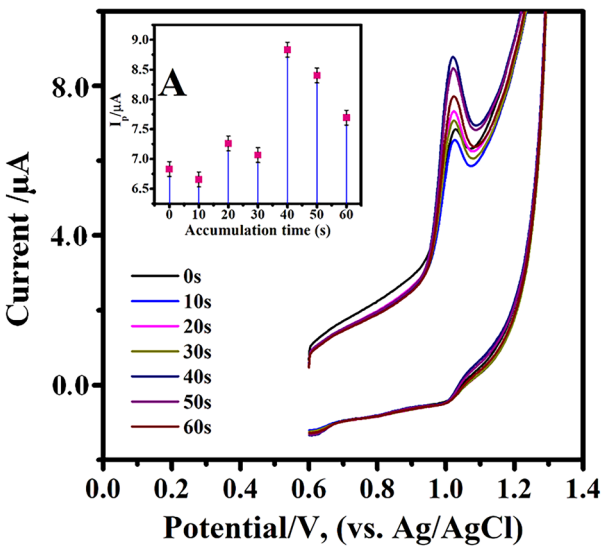

Fig. 1 Cyclic voltammograms of 0.1 mM CBM at poly(VVR)/GCE at 0.05 mV/s in 0.2 M PB 3.0 pH. **A** Inset of accumulation time (i.e., 0 s, 10 s, 20 s, 30 s, 40 s, 50 s, and 60 s) for 0.1 mM CBM against anodic peak current

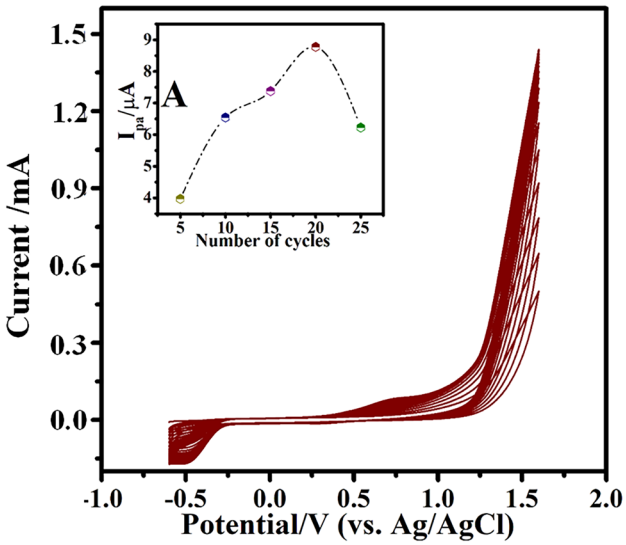

Fig. 2 Cyclic voltammogram of poly(VVR) film modified GCE. Scan rate: 0.1 V/s; C $_{(VVR)}$: 1.0 mM; supporting electrolyte: a mixture of 1.0 M NaOH and 1.0 $NaHSO_3$. **A** Anodic peak current plotted against the number of cycles of polymerization

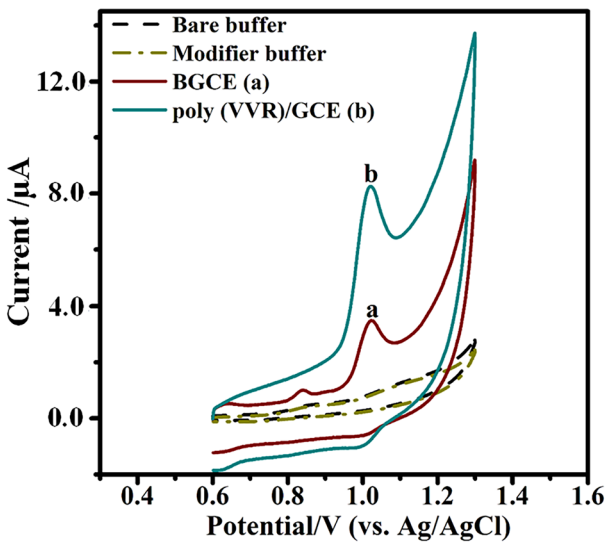

Fig. 3 Cyclic voltammograms at the BGCE (**a**), at poly(VVR)/GCE (**b**) in the presence of 0.1 mM CBM at 0.05 V/s in 3.0 pH PB at 40-s accumulation time

Electro-analytical Activity of CBM

The behavior of a 0.1 mM CBM fungicide at a developed GCE was studied using a CV technique at a bare glassy carbon electrode (BGCE) and at a poly(VVR)/GCE at a sweep rate of 50 mV/s in a pH of 3.0 PB at an accumulation time of the 40 s. In the presence of CBM at bare and at modified GCE, one intense oxidation peak and one reduction peak were observed. The anodic peak current at the poly(VVR)/GCE is 8.25 µA and at the bare GCE is 3.50 µA (Fig. 3). Also, there was a slight shift in the peak potential value. This kind of response is due to the electrocatalytic characteristics of the VVR dye. The peak potential (E_p) at bare GCE is 1.022 V, whereas the peak potential at poly(VVR)/GCE is 1.018 V. The electrode's excellent surface area exposes the GCE's active structure. The properties such as anti-fouling characteristics, large specific surface area, outstanding electrical conductivity, electro-catalytic effect, fast electron transmission capability, and remarkable chemical stability are enhanced by the excellent performance of CBM fungicide on poly(VVR)/GCE. Hence, further investigation of CBM was carried out using modified GCE.

The pH Effect Study

Examining toxic chemical molecules' electrochemical process is significant to understand better the reaction process, the speed, and the protons involved. The pH of a buffer solution is a vital research parameter that can affect the transfer of electrons from CBM and how it behaves electrochemically at poly(VVR)/GCE. The electrochemical reaction of 0.1 mM CBM at poly(VVR)/GCE at 40-s accumulation time with a scan rate of 50 mV/s within a pH 3.0–11.2 PB (0.2 M) was recorded using the CV technique. PB is treated as an inert electrolyte in the analysis with strong solvability in water and particular buffer resistance. It justifies the role of protons throughout the process. In the CBM molecule, the highest anodic peak current recorded was at 3.0 pH (Fig. 4) of its buffer solution.

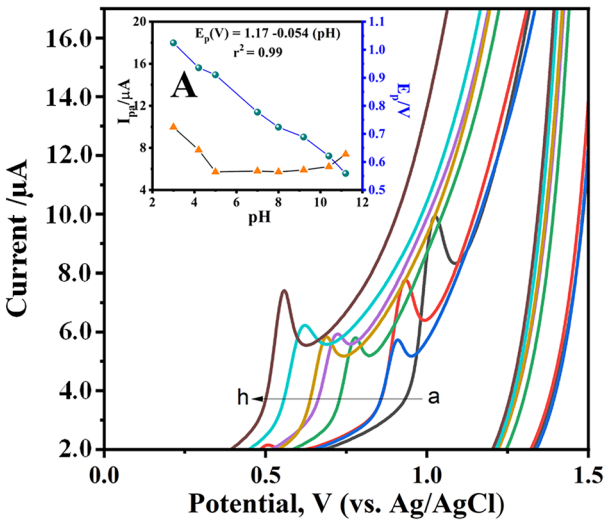

Fig. 4 CVs in the presence of 0.1 mM CBM at varying pH of PB at a poly(VVR)/GCE, (a–i; 3, 4.2, 5, 7, 8, 9.2, 10.4, 11.2) at an accumulation time of the 40 s at 50 mV/s scan rate. **A** I_{pa} and E_{pa} values plotted against pH values

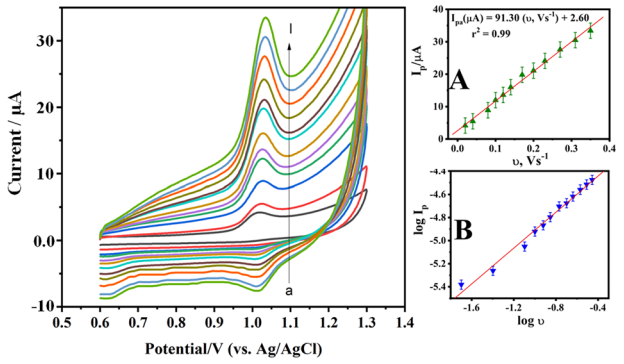

Fig. 5 The influence of varying scan frequencies (a–l in V/s; 0.02, 0.04, 0.08, 0.1, 0.12, 0.14, 0.17, 0.20, 0.23, 0.27, 0.31, 0.35) at poly(VVR)/GCE at 40-s accumulation time in the involvement of 0.2 M 3.0 pH PB by CV technique for 0.1 mM CBM. **A** I_{pa} plotted against scan rates. **B** Log I_p plotted against log υ

Moreover, in the graph of E_p vs. pH, the linearity is expressed as $E_p(V) = 1.170–0.054$ (pH); $r^2 = 0.996$; with pHs, increased linearity of peak potential was achieved (Fig. 4A). The slope of 0.054 is nearer to the Nernst equation value (0.059 E_p/pH), showing equal numbers of protons and electrons in the electro-oxidation reaction. As a result, throughout the research work, pH 3.0 was considered the ideal pH for the buffer solution.

Scan Rate Impact

The electrochemical process of the CBM fungicide was well understood at the poly(VVR)/GCE by analyzing the variation of scanning levels. The impact of the scan rate on 0.1 mM CBM oxidation in 0.2 M PB of pH 3.0 with an accumulation time of 40 s was assessed using a CV technique at poly(VVR)/GCE (Fig. 5). The Laviron equation is followed for the poly(VVR)/GCE and noted an improvement in the peak current and a reposition in the peak potential with a sweep rate. A linear increase in the maximum peak current was observed with sweep rate increase, for which the linear relationship is expressed as $I_p(\mu A) = 91.30$ (υ, V/s) + 2.60; $r^2 = 0.99$ (Fig. 5A). The plot of the log of anodic peak current versus the log scan rate is shown as input to ensure the electrode process. The linear regression expression is presented with log $I_p(\mu A) = 0.77$ (log υ, V/s) − 4.13; $r^2 = 0.99$ (Fig. 5B). The slope value is 0.77; this indicates that the electrode process is combined with adsorption and diffusion-controlled process. The Laviron Eq. (1) [36, 37] represents the relationship between scanning rate and anodic peak potential for an electrode reaction.

$$E_P = E^0 + \left(\frac{2.303RT}{(1-\alpha)nF}\right)\log\left(\frac{(1-\alpha)nF}{RTk^0}\right) + \left(\frac{2\cdot 303RT}{(1-\alpha)nF}\right)\log\ \upsilon \tag{1}$$

Within the electrode's process, the involvement of electrons is shown by n, υ is the sweep rate, and α is its charge transfer coefficient, whereas k^0 shows the heterogeneous rate constant at standard conditions and E^0 represents the formal redox potential. The heterogeneous constant, k^0, was estimated as 2.73 s^{-1}.

$$\Delta E_p = E_p - E_{P/2} = \frac{47\cdot 7}{\alpha n} \tag{2}$$

The Bard and Faulkner Formula (2) determines the value of αn as 1.41, and α was found to be equal to 0.58. In this, $E_{p/2}$ represents half of the peak potential, where current is proportional to half the maximum peak value of the current. The electrons and protons participated in the electro-oxidation process of about 2.0. This was estimated using the Bard and Faulkner expression alpha value for the

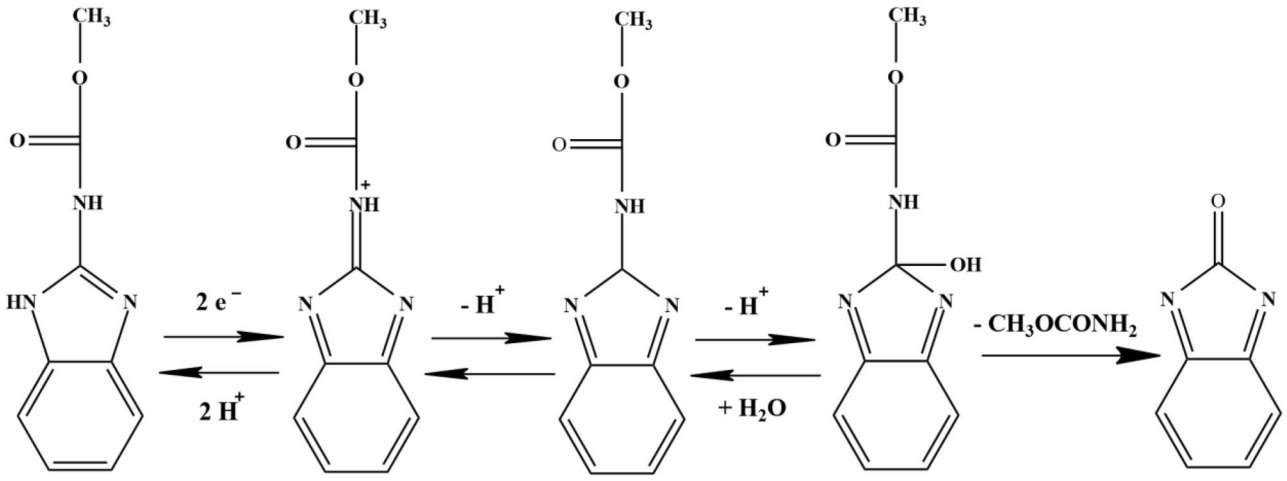

Scheme 1 Possible electro-oxidation mechanism of CBM

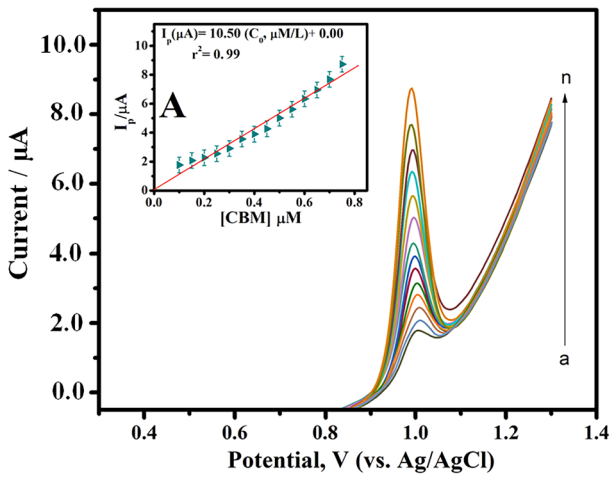

Fig. 6 DPVs recorded for different concentrations of CBM at accumulation time 40 s in 3.0 pH PB (a–n in µM; 0.05, 0.1, 0.15, 0.2, 0.25, 0.3, 0.35, 0.4, 0.45, 0.5, 0.55, 0.6, 0.65, 0.7). **A** Inset graph of I_{pa}/µA versus [CBM]/µM

CBM molecule at poly(VVR)/GCE. A possible electro-oxidation mechanism of CBM is shown in Scheme 1.

Analytical Applications

CBM Concentration

The DPV technique was used to obtain the peaks of good resolution at lower analyte concentrations. CBM concentrations varied from 0.05 to 0.7 µM to determine the sensitivity of poly(VVR)/GCE in 3.0 pH of PB at 40-s accumulation time (Fig. 6). Linear relationship achieved according to $I_p(\mu A) = 10.50\ (C_0, \mu M/L) + 1.28$; $r^2 = 0.99$, with its current value compared to the CBM concentration range. From the formulas, LOD = 3*S*/*M* and LOQ = 10*S*/*M*, the detection limit and the quantity limit have been calculated. Here, *S* indicates blank standard deviation, and *M* indicates the slope of the graph. The detection limit for this activity is 0.31×10^{-8} M. All previously reported LOD values can be seen in Table 1. The findings of LOD and LOQ from fabricated electrode showed low value indicating that it has excellent sensitivity, effective for CBM detection and determination [39–44].

Analysis of Soil Samples

Testing of soil samples was performed to influence the environmental and agricultural use of the generated electrode. The established sensor is sensitive to CBM analysis results based on Table 2. The SWV method was used at ambient temperature for CBM molecule studies. The recovery percentage is 90.00% and 99.00%.

Analysis of Water Samples

Water sample analysis was carried out to determine the presence of CBM in the water sample using the SWV method. Pre-treated water samples were then taken with a known CBM concentration to test the detection of CBM analysis. Table 3 shows the test results for other water samples. The recovery percentage is 90.00% and 100%.

Impact of Temperature Variation

Using a CV method, the effect of temperature on the electro-oxidation of CBM analyte was studied at poly(VVR)/GCE in 3.0 pH PB for the 40 s at a scan rate of 50 mV/s. The current values of CBM are elevated linearly due to the temperature being enhanced between 288 and 313 K with a decrease in peak current, which can be seen in Fig. 7. For thermodynamic expressions 3 and 4, the log (I_{pa}) of CBM vs. 1/temperature is linear. Due to the diffusibility differences of the CBM molecule, there is an increase in current oxidation (Eq. 3). As the temperature rises, the GCE-generated behavior plays an essential role in the activation energy,

Table 1 LOD comparison with other modified electrodes

Sl. No.	Modified electrode	Technique	LOD	References
1	ZMCPE	SWV	3.51 nmol/L	[38]
2	Nanoporous copper-reduced graphene oxide-GCE	DPV	0.09 µM	[39]
3	Boron-doped diamond electrode	SWV	0.40 mg/L	[40]
4	Silicon dioxide-multi-walled carbon nanotubes-GCE	SWV	0.05 µmol/L	[33]
5	La-doped Nd_2O_3-CPE	DPV	0.02 µM	[41]
6	Nanoporous gold-GCE	DPV	0.24 µM	[42]
7	β-Cyclodextrin-multiwalled carbon nanotubes-boron doped diamond electrode	SWAdSV	1.96×10^{-7} mol/L	[43]
8	Tricresyl phosphate-CPE	DPAdSV	0.20 mol/L	[44]
9	Poly(VVR)/GCE	DPV	0.31×10^{-8} M	Present work

Table 2 Determination of CBM in spiked soil samples

Sample	Spiked (μM)	Detected (μM)	Recovery (%)	RSD (%)
Black soil	0.1	0.09	90	4.84
	0.5	0.49	98	4.45
	1.0	0.97	97	4.50
Red soil	0.1	0.09	90	2.93
	0.5	0.47	94	2.81
	1.0	0.95	95	2.80
Brick soil	0.1	0.09	90	4.20
	0.5	0.48	96	3.94
	1.0	0.97	97	0.58
Lake soil	0.1	0.09	99	0.59
	0.5	0.49	98	0.58
	1.0	0.99	99	0.58
Agricultural soil	0.1	0.09	96	1.80
	0.5	0.48	96	1.80
	1.0	0.99	99	1.74

i.e., E_a, for the distribution of the CBM molecule. Using the anodic peak current of the CBM molecule, the Arrhenius equation was used to determine that the activation energy was 11.19 kJ/mol.

$$\sigma = \sigma^0 e^{-\frac{E_a}{RT}} \tag{3}$$

$$D = D^0 e^{-\frac{E_a}{RT}} \tag{4}$$

Here, conductivity/diffusibility is σ/D, the activation energy is E_a, σ^0/D is standard conductivity/initial diffusibility, the temperature is T, and the universal gas constant

Table 3 Finding of CBM in spiked water samples

Sample	Added (μM)	Found (μM)	Recovery (%)	RSD (%)
Lake water	0.1	0.09	90	1.70
	0.5	0.46	92	1.66
	1.0	0.93	93	1.64
Dam water	0.1	0.09	90	3.84
	0.5	0.48	96	3.60
	1.0	0.96	96	3.60
RO water	0.1	0.09	90	3.40
	0.5	0.47	94	3.25
	1.0	0.96	96	3.18
Pond water	0.1	0.10	100	1.00
	0.5	0.49	98	1.02
	1.0	0.99	99	1.01
Tap water	0.1	0.09	90	5.13
	0.5	0.49	98	4.71
	1.0	0.98	98	4.71

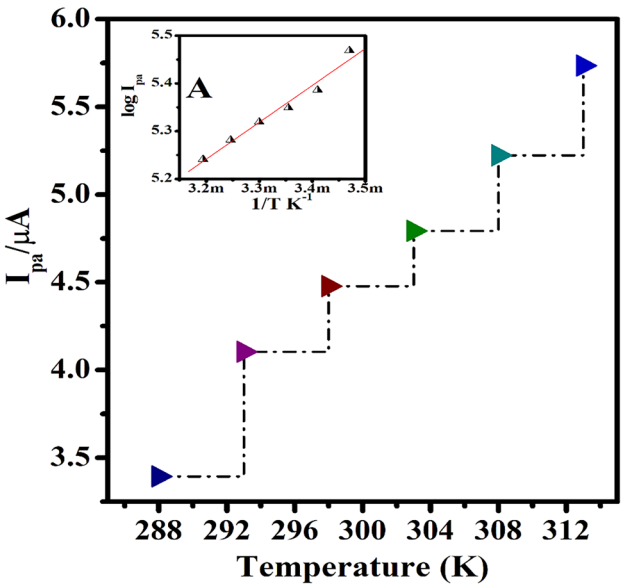

Fig. 7 Impact of varying temperatures (288 K, 293 K, 298 K, 303 K, 308 K, and 313 K) on 0.1 mM CBM anodic peak current at poly(VVR)/GCE in 3.0 pH PB. **A** Inset graph of log (I_{pa}) plotted against 1/T

is R (8.314 J mol^{-1} k^{-1}). In a practical means of investigating the applications, parameters must be conducted at ambient temperature, even though the peak current of the analyte increases as the temperature goes high [45, 46]. With the Erying equation as well as the thermodynamic equations, the change in enthalpy (H^*) and entropy (S^*) of CBM at poly(VVR)/GCE was calculated:

$$\Delta G^* = -RT \ln\left(\frac{kh}{Tk_B}\right) \tag{5}$$

$$\Delta H^* = \Delta G^* + T\Delta S^* \tag{6}$$

Variable H^* is utilized to determine whether the electrode reaction is spontaneous. For S^* positive variable, G^* negative, and H^* negative based upon the Gibbs free energy [47–49]. The Boltzmann constant, k_B (1.381×10^{-23} m^2 kg s^{-2} k^{-1}), and the Planck constant, h (6.66×10^{-34} J s), are also included in the above 6 and 7 equations. As polymerization of VVR was carried out, the working electrode expedited the processes like an electrocatalyst which increased the current in the system. The E_a^* value, as well as the thermodynamic variables, are listed in Table 4.

Selectivity of the Poly(VVR)/GCE

Selectivity of the electrode is identifying specific molecules or ions in the presence of other molecules or ions. Since the sensor is frequently used to detect a molecule or ion in a mixture of all other ions or molecules, it is a crucial parameter to consider when applied to study the actual samples.

Table 4 Thermodynamic parameters of CBM at poly(VVR)/GCE

Thermodynamic parameters	Obtained values
E_a* (kJ mol^{-1})	11.19
ΔH* (kJ mol^{-1})	8.72
ΔS* (kJ mol^{-1})	−225.52
ΔG* (kJ mol^{-1})	75.92

It has been discovered that the modified electrode is very sensitive to the CBM chemical. By analyzing the interference effect with various interfering metal ions (1.0 mM), such as calcium chloride, copper sulphate, ferrous sulphate, potassium nitrate, manganese sulphate, and zinc chloride, the electrochemical performance of CBM at poly(VVR)/GCE was studied using the SWV technique. Considering the 100-fold metal ion concentrations, there was no interference in the CBM peak potential, indicating that the suggested approach possesses a higher selectivity for CBM detection.

Repeatability and Reproducibility of the Poly(VVR)/GCE

The essential parameters for assessing the sensitivity and reliability of the fabricated working electrode are reproducibility and repeatability. Reproducibility of poly(VVR)/GCE was tested by preserving the electrode in a closed area for approximately 20 days. At ambient temperature, the reproducibility was processed on that same day, and its RSD was found to be 1.97%, indicating that the electrode shows excellent reproducibility. Repeatability has been achieved in ideal circumstances so far. The repeatability interaction was set up by five consecutive 0.1 mM CBM standard solution estimations. The poly(VVR)/GCE maintained 98% of the initial peak current, confirming the stability of the fabricated poly(VVR)/GCE. So, the fabricated poly(VVR)/GCE is suitable for long-term consistency and reproducibility for analytical applications.

Conclusions

The proposed work focuses on developing a simple and effective poly(VVR)/GCE working electrode for detecting and determining CBM. With the poly(VVR)/GCE, nanomolar CBM detection was performed. Due to the electropolymerization of the VVR and its layer growth on the GCE, an increased peak current of CBM was observed, double the peak current of CBM at a bare GCE. The electrode process was observed to be quasi-reversible. Vat dyes are the vital dyes commonly employed for printing, which include dyeing cellulosic fibers and cotton. The VVR dye has been used as a modifier of GCE electro-polymerization. The fabricated electrode showed CBM sensing and quantification in actual samples. The sensor has successfully demonstrated the detection limit, high sensitivity, quick reaction, reproducibility, electro-catalytic performance, and repeatability. The fabricated poly(VVR)/GCE revealed a minimum detecting limit of 0.312×10^{-8} M for the CBM analyte. Based on the temperature variation effect, activation energy and other thermodynamic variables like ΔS*, ΔH*, and ΔG* have been investigated.

Declarations

Competing Interests The authors declare no competing interests.

References

1. V.K. Gupta, A.K. Singh, M. Al Khayat, B. Gupta, Neutral carriers based polymeric membrane electrodes for selective determination of mercury (II), Analytica Chimica Acta. **590**, 81–90 (2007)
2. A.K. Jain, V.K. Gupta, L.P. Singh, J.R. Raisoni, A comparative study of Pb2+ selective sensors based on derivatized tetrapyrazole and calix[4]arene receptors. Electrochim. Acta **51**, 2547–2553 (2006)
3. N.P. Shetti, M.M. Shanbhag, S.J. Malode, R.K. Srivastava, K.R. Reddy, Amberlite XAD-4 modified electrodes for highly sensitive electrochemical determination of nimesulide in human urine. Microchem. J. **153**, 104389 (2020)
4. K.K. Prabhu, S.J. Malode, N.P. Shetti, R.M. Kulkarni, Analysis of herbicide and its applications through a sensitive electrochemical technique based on MWCNTs/ZnO/CPE fabricated sensor. Chemosphere **287**, 132086 (2022)
5. N.P. Shetti, S.J. Malode, D.S. Nayak, K.R. Reddy, Novel heterostructured Ru-doped TiO_2/CNTs hybrids with enhanced electrochemical sensing performance for Cetirizine. Materials Research Express. **6**(11), 115085 (2019)
6. K.K. Prabhu, S.J. Malode, R.M. Kulkarni, N.P. Shetti, Electrochemical investigations-based on ZnO@Cu core–shell in presence of CTAB surfactant for 4-Chlorophenol. Environ. Technol. Innov. **24**, 102029 (2021)
7. S. Erogul, S.Z. Bas, M. Ozmen, S. Yildiz, A new electrochemical sensor based on Fe3O4 functionalized graphene oxide-gold nanoparticle composite film for simultaneous determination of catechol and hydroquinone. Electrochim. Acta **186**, 302–313 (2015)
8. Y. Wang, Y. Xiong, J. Qu, J. Qu, S. Li, Selective sensing of hydroquinone and catechol based on multiwalled carbon nanotubes/polydopamine/gold nanoparticles composites. Sens. Actuators, B Chem. **223**, 501–508 (2016)
9. S. El Aggadi, N. Loudiyi, A. Chadil, Z. El Abbassi, A. El Hourch, Electropolymerization of aniline monomer and effects of synthesis conditions on the characteristics of synthesized polyaniline thin films, Mediterranean. J. Chem. **10**, 138–145 (2020)
10. I. Suresh, S. Selvaraj, N. Nesakumar, J.B. Balaguru Rayappan, A.J. Kulandaiswamy, Nanomaterials based non-enzymatic electrochemical and optical sensors for the detection of carbendazim: A review, Trends in Environmental Analytical Chemistry, **31**, 00137 (2021)
11. S. Šekuljica, V. Guzsvany, J. Anojčić, T. Hegedűs, M. Mikov, K. Kalcher, Imidazolium-based ionic liquids as modifiers of carbon paste electrodes for trace-level voltammetric determination

of dopamine in pharmaceutical preparations. J. Mol. Liq. **306**, 112900 (2020)
12. G. Inzelt, M. Pineri, J.W. Schultze, M.A. Vorotyntsev, Electron and proton conducting polymers: recent developments and prospects. Electrochim. Acta **45**, 2403–2421 (2000)
13. C.G. Nan, Z.Z. Feng, W.X. Li, D.J. Ping, C.H. Qin, Electrochemical behavior of tryptophan and its derivatives at a glassy carbon electrode modified with hemin. Anal. Chim. Acta **452**, 245–254 (2002)
14. W. da Silva, A.C. Queiroz, C.M. Brett, Nanostructured poly (phenazine)/Fe2O3 nanoparticle film modified electrodes formed by electropolymerization in ethaline-deep eutectic solvent. Microscopic and electrochemical characterization, Electrochimica Acta. **347**, 136284 (2020)
15. C.-X. Xu, K.-J. Huang, Y. Fan, Z.-W. Wu, J. Li, Electrochemical determination of acetaminophen based on TiO_2–graphene/poly(methyl red) composite film modified electrode. J. Mol. Liq. **165**, 32–37 (2012)
16. A. Yamuna, T.-W. Chen, S.-M. Chen, Synthesis and characterizations of iron antimony oxide nanoparticles and its applications in electrochemical detection of carbendazim in apple juice and paddy water samples. Food Chem. **373**, 131569 (2022)
17. W. Zhong, F. Gao, J. Zou, S. Liu, M. Li, Y. Gao, Y. Yu, X. Wang, L. Lu, MXene@Ag-based ratiometric electrochemical sensing strategy for effective detection of carbendazim in vegetable samples. Food Chem. **360**, 130006 (2021)
18. W. Jin, L. Ruiyi, L. Nana, S. Xiulan, Z. Haiyan, W. Guangli, L. Zaijun, Electrochemical detection of carbendazim with mulberry fruit-like gold nanocrystal/multiple graphene aerogel and DNA cycle amplification. Microchim. Acta **188**, 284 (2021)
19. X.B. Joseph, J.N. Baby, S.-F. Wang, B. Sriram, M. George, Interfacial superassembly of Mo_2C@NiMn-LDH frameworks for electrochemical monitoring of carbendazim fungicide. ACS Sustainable Chemistry & Engineering **9**, 14900–14910 (2021)
20. R. Liu, Y. Chang, F. Li, V. Dubovyk, D. Li, Q. Rand, H. Zhao, Highly sensitive detection of carbendazim in juices based on mung bean-derived porous carbon@chitosan composite modified electrochemical sensor. Food Chem. **392**, 133301 (2022)
21. G.A.F. Mekeuo, C. Despas, C.P.N.-Njiki, A. Walcarius, E. Ngameni, Preparation of functionalized Ayous sawdust-carbon nanotubes composite for the electrochemical determination of carbendazim pesticide, Electroanalysis, **34**, 667–676 (2022)
22. Y. Li, X. Chen, H. Ren, X. Li, S. Chen, B.-C. Ye, A novel electrochemical sensor based on molecularly imprinted polymer-modified C-ZIF67@Ni for highly sensitive and selective determination of carbendazim. Talanta **237**, 122909 (2022)
23. M.B. Heyman, S.A. Abrams, H.S.O. Gastroenterology, Committee on Nutrition. Fruit juice in infants, children, and adolescents: current recommendations. Pediatrics **139**, e20170967 (2017)
24. M.V. Sant'Anna, S.W. Carvalho, A. Gevaerd, J.O. Silva, E. Santos, I.S. Carregosa, A. Wisniewski Jr, L.H. Marcolino-Junior, M.F. Bergamini, E.M. Sussuchi, Electrochemical sensor based on biochar and reduced graphene oxide nanocomposite for carbendazim determination, Talanta **220**, 121334 (2020)
25. S.-Y. Wang, X.-C. Shi, F.-Q. Liu, P. Laborda, Chromatographic methods for detection and quantification of carbendazim in food, Journal of Agricultural and Food. Chemistry **68**, 11880–11894 (2020)
26. M.A. Daam, M.V. Garcia, A. Scheffczyk, J. Römbke, Acute and chronic toxicity of the fungicide carbendazim to the earthworm Eisenia fetida under tropical versus temperate laboratory conditions. Chemosphere **255**, 126871 (2020)
27. S.T. McBeath, D.P. Wilkinson, N.J.D. Graham, Application of boron-doped diamond electrodes for the anodic oxidation of pesticide micropollutants in a water treatment process: a critical review. Environ. Sci.: Water Res. Technol. **5**, 2090–2107 (2019)
28. Y. Guo, S. Guo, J. Li, E. Wang, S. Dong, Cyclodextrin–graphene hybrid nanosheets as enhanced sensing platform for ultrasensitive determination of carbendazim. Talanta **84**, 60–64 (2011)
29. N.L. Pacioni, V.N.S. Occello, M. Lazzarotto, A.V. Veglia, Spectrofluorimetric determination of benzoimidazolic pesticides: effect of p-sulfonatocalix [6] arene and cyclodextrins. Anal. Chim. Acta **624**, 133–140 (2008)
30. S. Jiao, J. Jin, L. Wang, Tannic acid functionalized N-doped graphene modified glassy carbon electrode for the determination of bisphenol A in food package. Talanta **122**, 140–144 (2014)
31. P. Manisankar, P.A. Sundari, R. Sasikumar, S.P. Palaniappan, Electroanalysis of some common pesticides using conducting polymer/multiwalled carbon nanotubes modified glassy carbon electrode. Talanta **76**, 1022–1028 (2008)
32. O.D. Renedo, M.A. Alonso-Lomillo, M.A. Martinez, Recent developments in the field of screen-printed electrodes and their related applications. Talanta **73**, 202–219 (2007)
33. C.A. Razzino, L.F. Sgobbi, T.C. Canevari, J. Cancino, S.A. Machado, Sensitive determination of carbendazim in orange juice by electrode modified with hybrid material. Food Chem. **170**, 360–365 (2015)
34. S.K. Patra, A.K. Patra, P. Ojha, N.S. Shekhawat, A. Khandual, Vat dyeing at room temperature. Cellulose **25**, 5349–5359 (2018)
35. J.R. Aspland, Vat dyes and their application. Textile Chem. Color. **24**, 22 (1992)
36. A. Bard, L. Faulkner, J. Leddy, C. Zoski, *Electrochemical methods: fundamentals and applications*, vol. 2 (Wiley, New York, 1980), p.231
37. E. Laviron, General expression of the linear potential sweep voltammogram in the case of diffusionless electrochemical systems. J. Electroanal. Chem. Interfacial Electrochem. **101**(1), 19–28 (1979)
38. E.M. Maximiano, F. de Lima, C.A.L. Cardoso, G.J. Arruda, Modification of carbon paste electrodes with recrystallized zeolite for simultaneous quantification of thiram and carbendazim in food samples and an agricultural formulation. Electrochim. Acta **259**, 66–76 (2018)
39. C. Tian, S. Zhang, H. Wang, C. Chen, Z. Han, M. Chen, Y. Zhu, R. Cui, G. Zhang, Three-dimensional nanoporous copper and reduced graphene oxide composites as enhanced sensing platform for electrochemical detection of carbendazim. J. Electroanal. Chem. **847**, 113243 (2019)
40. T. Lima, H.T.D. Silva, G. Labuto, F.R. Simões, L. Codognoto, An experimental design for simultaneous determination of carbendazim and fenamiphos by electrochemical method. Electroanalysis **28**, 817–822 (2016)
41. Y. Zhou, Y. Li, P. Han, Y. Dang, M. Zhu, Q. Li, Y. Fu, A novel low-dimensional heteroatom doped Nd2O3 nanostructure for enhanced electrochemical sensing of carbendazim. New J. Chem. **43**, 14009–14019 (2019)
42. X. Gao, Y. Gao, C. Bian, H. Ma, H. Liu, Electroactive nanoporous gold driven electrochemical sensor for the simultaneous detection of carbendazim and methyl parathion. Electrochim. Acta **310**, 78–85 (2019)
43. M. Brycht, O. Vajdle, K. Sipa, J. Robak, K. Rudnicki, J. Piechocka, A. Tasić, S. Skrzypek, V. Guzsvány, β-Cyclodextrin and multiwalled carbon nanotubes modified boron-doped diamond electrode for voltammetric assay of carbendazim and its corrosion inhibition behavior on stainless steel. Ionics **24**, 923–934 (2018)
44. A.M. Ashrafi, J. Đorđević, V. Guzsvány, I. Švancara, T. Trtić-Petrović, M. Purenović, K. Vytřas, Trace determination of carbendazim fungicide using adsorptive stripping voltammetry with a carbon paste electrode containing tricresyl phosphate. Int. J. Electrochem. Sci. **7**, 9717–9731 (2012)
45. N.P. Shetti, S.J. Malode, S.D. Bukkitgar, G.B. Bagihalli, R.M. Kulkarni, S.B. Pujari, K.R. Reddy, Electro-oxidation and

determination of nimesulide at nanosilica modified sensor. Materials Science for Energy Technologies **2**(3), 396–400 (2019)
46. S.J. Malode, K. Prabhu, B.G. Pollet, S.S. Kalanur, N.P. Shetti, Preparation and performance of WO_3/rGO modified carbon sensor for enhanced electrochemical detection of Triclosan. Electrochim. Acta **429**, 141010 (2022)
47. S.J. Malode, N.P. Shetti, K.R. Reddy, Highly sensitive electrochemical assay for selective detection of Aminotriazole based on TiO_2/poly(CTAB) modified sensor. Environ. Technol. Innov. **21**, 101222 (2021)
48. W.T. Tan, J.K. Goh, Electrochemical oxidation of methionine mediated by a fullerene-C60 modified gold electrode. Electroanalysis **20**, 2447–2453 (2008)
49. S.J. Malode, N.P. Shetti, S.T. Nandibewoor, Os(VIII)/Ru(III) catalysed oxidation of l-valine by Ag(III) periodate complex in aqueous alkaline medium: a comparative kinetic study. Catal. Lett. **141**(10), 1526–1540 (2011)